Superelastic NiTi Thin Film Small Vessel Graft For Vascular Repair

Youngjae Chun[a], Daniel S. Levi[b], K. P. Mohanchandra[a], Gregory P. Carman[a]

[a]Department of Mechanical and Aerospace Engineering, University of California, Los Angeles, CA,32-135, Engineering Ⅳ, Los Angeles, CA 90095

[b]Pediatric Cardiology, Mattel Children's Hospital, University of California, Los Angeles, B2-427, 10833 Le Conte Avenue, Los Angeles, CA 90095-1743

ABSTRACT

NiTi thin film produced by sputter deposition was used in the design of small vessel grafts intended to treat small vessel aneurysms. Thin film small vessel grafts were fabricated by "hot-target" DC sputter deposition. Both stress-strain curves and DSC curves were generated for the film used to fabricate small vessel grafts. The films used for small vessel grafts had an A_f temperatures of approximately 36°C allowing for body activated response from a micro-catheter. Thin film small vessel grafts were tested in a pulsatile flow loop *in-vitro*. Small vessel grafts could be compressed into and easily delivery in < 3Fr catheters. Theoretical frictional and wall drag forces on a NiTi thin film small vessel vascular graft were calculated and the radial force exerted by thin film small vessel grafts was evaluated theoretically and experimentally. *In-vivo* studies in swine confirmed that NiTi thin film small vessel grafts could be deployed accurately and consistently in the swine vascular system.

Key words: small vessel graft, NiTi, thin film, aneurysm, transcatheter.

1. INTRODUCTION

An aneurysm is a spherical out-pouching of blood vessels formed from a localized weakness in the wall of an artery. Aneurysms can occasionally rupture and cause a life threatening hemorrhage. Postmortem examinations indicate that 10~12 million people have brain aneurysms in the United States [1] and 20~50% will potentially rupture [2]. Aneurysm rupture carries a high rate of morbidity and mortality [3]. Current approaches to prevent aneurysms from rupturing include both surgical and transcatheter methods.

A surgical approach to treat aneurysms by "clipping" the aneurysm neck was developed by Walter Dandy in 1936 and proved to be an effective treatment for a select group of aneurysms [1]. However, this procedure requires a craniotomy (an opening in the skull) and is not always applicable depending on the aneurysm size, location and complexity. More recently, transcatheter procedures to treat vascular aneurysms have been developed. Guglielmi *et al.* introduced an endovascular therapy using platinum coils to fill the aneurysm sac in 1990 [4, 5]. Because this coil embolization technique is less invasive

and more cost-effective than surgery, it has become the standard of care for most aneurysms. These coils pack the aneurysm sac densely to limit blood flow in the aneurysm and produce more local thrombosis within the aneurysm.

While coils are beneficial, they can only be used for aneurysms with "necks" narrow enough to hold coils in the aneurysm. To address this issue, a stent can be placed across the neck of a broad-neck aneurysm and coils placed into the aneurysm through the cells of the stent. This procedure is complicated (it involves two types of devices - a stent and multiple coils) and is limited by the physical size of the stent's delivery system [6-14]. The ideal device for treatment of aneurysms would be a "covered" stent graft which occludes the neck of both narrow and broad necked aneurysms. "Covered stent grafts" have traditionally been conventional mesh type stents wrapped in ePTFE (polytetrafluoroethylene). While they can wall off aneurysms by circumferentially covering the wall of an artery, they have been far too bulky for use as small vessel grafts. A low profile covered stent graft for the treatment of aneurysms in small, tortuous vessels has yet to be fully evaluated *in-vivo* or *in-vitro*.

This paper demonstrates analytically as well as with *in-viv*o and *in-vitro* demonstrations that a NiTi thin film device represents a plausible low profile covered small vessel graft (or stent). The NiTi thin film was produced by a hot target sputter deposition process [15] with austenite finish temperatures slightly below body temperatures. Previous work has demonstrated the excellent corrosion resistance of NiTi thin film [16]. An analytical model is derived to predict the drag force on the film in the vascular system as well as the frictional forces with the vascular wall. *In-vitro* tests validate the predictions and the ability of the small vessel graft to be immobilized. Radio opaque markers are attached to the thin film and *in-vivo* tests demonstrate the deployment without migration of the thin film small vessel grafts in a swine vascular system. *In-vivo* tests also evaluate endothelial cell growth on the implanted NiTi thin film grafts.

2. ANALYSIS

The basic concept of a NiTi thin film small vessel graft is presented in Fig. 1: a sheet of NiTi thin film (4~10μm thick) is initially tightly rolled and placed into a small diameter catheter (e.g., 0.69mm ID). The stresses induced in the film cause the material to become martensitic (i.e. stress induced phase transformation) and more malleable when compared to the austenitic film. Using an endovascular procedure, the catheter is guided through the vascular system to the aneurysm location over a 0.014 inch (0.36mm in diameter) guidewire. The thin film is subsequently pushed out of the catheter and deploys conformally with the artery as shown in Fig. 1 (A). When pushed out into the blood stream, the thin film reverts to the higher stiffness austenite phase causing it to conformally deploy against the vascular blood vessel.

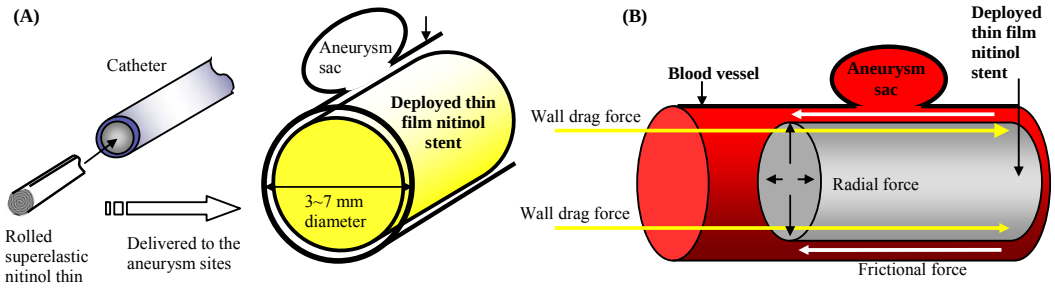

Fig. 1 Schematic diagram of a NiTi thin film small vessel graft: (A) for treatment of small vessel aneurysms and (B) force balance of NiTi thin film small vessel graft and blood flow

The small vessel graft must be able to occlude the aneurysm by completely wrapping around the vascular wall's interior without migrating after deployment or blocking flow through the vessel. Figure 1 (B) illustrates the forces present in a deployed thin film small vessel graft. The forces consist of radial forces, frictional forces, and hemodynamic shear forces. The radial forces induced during small vessel graft deployment produce frictional or holding forces between the graft and vascular wall. The blood flow through the graft interior introduces hemodynamic shear stress or a drag force on the thin film. A balance of these forces determines if the thin film small vessel graft remains immobilized or migrates in the vascular system.

A basic fluid mechanics model is used to approximate the hemodynamic shear stress induced on the thin film from blood flow. These calculations assume that the vessel is straight and the diameter is constant which limits the applicability of these results to some areas of the vascular system. The hemodynamic shear stress (τ_{wall}) is calculated using Poiseuille's Law assuming a straight vascular wall [17-19]. The total hemodynamic drag force on the film is

$$F_{Drag} = \tau_{wall} \cdot A = \left(\frac{4\mu Q}{\pi r^3} \right) \cdot (2\pi r l) = 8\pi\mu \cdot l \cdot v \qquad \text{Eq. (1)}$$

where μ is blood viscosity, Q is blood flow rate, r is artery radius, l is length (i.e., axial) of thin film small vessel graft, and v is velocity of blood flow. The velocity of fully developed pulsatile blood flow ranges between 0.5~1.0m/s in human CNS (Central Nervous System) arteries [20, 21], and the blood viscosity is approximately 0.004Ns/m^2 (4*centipoise*) [18]. The remaining two variables are functionally dependent upon artery size and thin film small vessel graft length. To immobilize the thin film small vessel graft, the frictional forces must be larger than the drag force. The frictional force is proportional to the radial force developed between the thin film and vascular wall.

Estimating radial force from the small vessel graft deployment is based on the assumption that the NiTi is thin, long and isotropic. Using these assumptions we argue that the deployment is similar to a long slender beam subjected to a internal bending moment. The radial force resultant (F_{Radial}) is subsequently

due to the bending moment produced by the NiTi unrolling in the austenite phase due to the shape memory effect. This radial force can be approximated by the following equation.

$$F_{Radial} = \left(\frac{E}{1-\nu^2} \cdot \frac{1}{24} \times h^3 \right) \cdot \frac{1}{r} \cdot \frac{w}{l} \qquad \text{Eq. (2)}$$

where w is width, E is Young's modulus of the austenite phase of NiTi ($83 \times 10^9 Pa$), ν is Poisson's ratio (ν=0.33), and h is thin film thickness. The frictional force between the vascular wall and the thin film is related to the radial force and coefficient of friction. Petrini *et al*. used a coefficient of friction (μ) of 0.05 to simulate the mechanical characteristics of a NiTi Coronary stent [22, 23]. As a reference, Ikeda *et al*. measured a friction coefficient of approximately 0.39 between pig arterial wall and polyethylene [24] and Dunn *et al.* showed a friction coefficient range of 0.03~0.06 between glass and endothelial cells [25]. In this study we chose a conservative friction coefficient of 0.05 between thin film NiTi surface and vascular wall to estimate the frictional force (i.e., $F_{friction} \propto \mu$).

3. FABRICATION

By using a near equiatomic alloy target, a DC sputtering technique was used to produce thin films of NiTi with an austenite finish temperature well below body temperature. The films were deposited on a 4″ silicon wafer covered with a 500nm thick silicon oxide buffer layer to prevent diffusion of nickel-titanium atoms into the silicon (i.e., to prevent silicide formation) and reduce or eliminate adhesion of the thin film to the silicon substrate [26]. Depositions were performed at a base pressure below $5 \times 10^{-8} Torr$ and Ar pressure of $1.5 \times 10^{-3} Torr$. The deposition rate was 0.1μm/min and several different thickness values were fabricated (i.e., t = 6, 8, 10, and 12μm thick). During deposition the target was heated and the substrate was translated in 80mm lengths perpendicular to the sputtering direction to minimize compositional variations. Based on prior measurements, the compositional variations were expected to be less than 1 *atomic%* within a 3″ diameter zone of the Si wafer [27]. The deposited film was removed from the substrate and the stand alone film was crystallized at 500°C for 120minutes in a vacuum less than $10^{-7} Torr$. A more detailed description of the film deposition and characterization is described by Ho *et al.* and Gill *et al.* [15, 28].

Following crystallization, the film was machined into rectangular sheets (t x 15mm x 15mm). Several approaches were used to roll the film and to insert the small vessel graft sheets into < 3Fr catheters (<0.69mm inner diameter). In all cases, small vessel grafts were rolled on 0.64mm steel cylinders. After carefully rolling the film with the cylinder, the rolled thin film is inserted into the delivery catheter and the cylinder is removed. *In-vitro* and *in-vivo* studies utilized neuroform delivery catheters (Boston Scientific, Natick, MA 3 Fr). After loading the thin film small vessel graft into the tip of this catheter, it was guided into position over a 0.014 inch guidewire. Deployment is then accomplished by removing the guidewire and simply pushing the small vessel graft out of the catheter with a 0.6mm OD "push wire".

For deployment in arteries larger than 4~5mm in diameter, calculations and preliminary *in-vitro* studies showed that our NiTi thin film small vessel graft on its own may have insufficient forces to prevent migration (radial force is inversely proportional to the radius). To address this issue, initially we developed larger diameter thin film sheets. These small vessel grafts provided a double-wrap design that would allow the film to wrap twice around the interior of the vessel. In addition to the double-wrap design, we produced small vessel grafts containing reinforced superelastic NiTi wire scaffoldings. Although three different skeletal structures were considered (Fig. 2), only the "zigzag" structure was tested *in-vivo*. The coil structure shown in Fig. 2 (A) was manufactured by winding a 0.13mm diameter superelastic NiTi wire around a cylinder approximating the radius of the arterial wall and heating at 500°C for 30minutes to shape set the NiTi wire. After hot shaping, the coil was physically pulled straight to induce a stress induced phase transformation and inserted into the delivery catheter containing the rolled small vessel graft (as described above). The coil was positioned such that there was equal length of coil before and after the rolled graft sheets. When deployed, one-third of the coil is initially pushed out of the catheter prior to deploying the thin film small vessel graft. Once the thin film portion of the stent is delivered, the remainder of the wire coil is deployed.

The "zigzag" structure (Fig. 2 (B) and (C)) was formed by setting 0.13mm diameter superelastic NiTi wire on a cylinder approximating the radius of the arterial wall and heating at 500°C for 30minutes to shape set. After hot shaping, the structure was physically compressed to induce a stress induced phase transformation and then inserted into the delivery catheter as described above for coil. Inside the catheter, the wire skeleton has 3~4mm of overhang length, before and after the rolled small vessel graft sheets. The supporting NiTi is designed to retain sufficient longitudinal flexibility to permit the catheter and structural backbone to navigate through a tortuous cerebral vascular system.

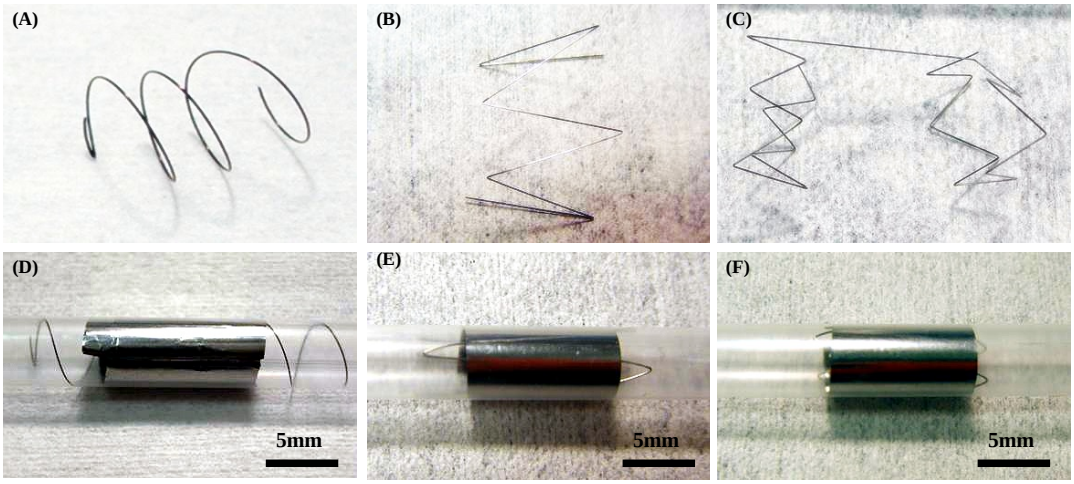

Fig. 2 Three different types of NiTi wire-based reinforcements: (A) coil, (B) single-zigzag design, (C) dual-zigzag design, and (D) ~ (F) deployed fashion respectively

Successfully deploying the stent at the aneurysm site requires an image-guided procedure requiring radiopaque material. The x-ray intensity in a material can be described by the absorption of photon in the media, which is defined by Lambert- Beers law;

$$I_x = I_0 e^{-\alpha \cdot \rho \cdot t} \qquad \text{Eq. (3)}$$

where I_0 is the intensity of the incident of x-ray source, I_x is the intensity of the x-ray exiting the material, α is mass absorption coefficient of the material, ρ is the mass density of the material, and t is the thickness of the material. Especially when working in vasculature structures encased in and close to bone, absorption and scattering of electrons is far from trivial [29]. The mass absorption coefficient of NiTi was calculated using the relative atomic mass and weight fraction of the Nickel and Titanium atoms and found to be 171.24. The density of NiTi material is 6.45g/cm^3 and standard intensity of the incident x-ray (I_0) for interventional procedures is approximately 50-70keV [30] with the system used in this study being equal to 70keV.

Using these values, it was determined that 130µm of NiTi represent a thickness easily imaged, i.e. I_x / I_0 was calculated to be 5.81×10^{-7}. While 130µm was the theoretical value, we also discovered that the 10 micron stents could also be seen faintly *in* vivo, however they were difficult to visualize with standard fluoroscopy. Thus, small tantalum markers (80µm x 150µm x 100µm) which have a higher density 16.6g/cm^2 when compared to NiTi were mechanically attached to the small vessel grafts for better visualization and placement of the small vessel graft. (Note that tantalum is well described to be a non-corrodable, biocompatible metal [31])

In addition to evaluating the NiTi thin film small vessel grafts, micro-patterning on thin film NiTi was investigated to improve flexibility and promote endothelialization through micro holes. Using a lift-off method and photolithography, 30x60µm diamond patterns were fabricated. The first step in the lift off method for producing patterned thin film NiTi is to create 50 micron deep trenches using photolithography and a deep reactive ion etching (DRIE) technique. Following this, a 500nm Cu sacrificial layer and a 500nm SiO_2 barrier layer are deposited by e-beam evaporation and PECVD techniques, respectively. The NiTi thin film is deposited by DC sputtering process onto the SiO_2. Cu and SiO_2 layers are removed and stand alone film is crystallized at 500°C for 120minutes in a vacuum of less than 1×10^{-7} *Torr*.

4. EXPERIMENTAL SETUP

Prior to manufacturing the small vessel grafts, both transformation temperatures and mechanical characteristics of the NiTi films were analyzed. Transformation temperatures were measured in a Shimazdu DSC-50 using approximately 10mg of NiTi thin film. Specimens were heated to 100°C and then cooled to -60°C at a constant rate of 7°C/min. From the endothermic and exothermic peaks of the DSC, the transformation temperatures (A_s, A_f, M_s and M_f) were determined using a slope line extension method. Rectangular sheets of NiTi thin film were also mechanically tested in MTS Tytron® mechanical

tester. Tests were conducted at both 22°C and 35°C. The tensile load was obtained from a load cell (resolution 0.1N) and relative grip displacements were measured (0.1μm resolution). Strain was calculated using the original distance (approximately 20mm) between the grips as a gage length producing an error less than 10% due to end/grip effects.

The deployment force of the NiTi sheets was measured in a specialized test setup on a vibration isolation table. A 5mm lumen plastic tube was cut in half along its axis to simulate the vascular geometry. The half plastic tube was placed over a force measurement system (1.0×10^{-5}N resolution) and a NiTi small vessel graft was deployed into the plastic tube to measure the small vessel graft's deployment force F_{radial} (see Eq. (2)). Four different thickness small vessel grafts (i.e., 6μm, 8μm, 10μm, and 12μm) were evaluated and each NiTi small vessel graft was tested five times.

A Harvard Apparatus pulsatile pump (Harvard Medical, Holliston, MA) was used to approximate flow in small arteries to allow for *in vitro* testing of small vessel graft delivery, deployment and stability. The flow loop was constructed with 5mm ID PVC tubing and the systole/diastole ratio was set to 40:60. The stroke volume was incrementally increased from 10cc to 30cc per stroke (600 to 2400cc/min) to allow for evaluation of the small vessel graft's resistance to migration with flow velocities from 0.5~2.0m/s. Prior to animal testing, all small vessel grafts were evaluated with multiple deployments in the pulsatile flow loop using the exact wires and delivery catheters.

In-vivo tests were conducted in accordance with a protocol approved by the UCLA Animal Research Committee. Two 25kg Yorkshire swine were prepared and draped in the usual sterile fashion. General anesthesia was administered via an endotracheal tube inserted via the direct laryngoscopy. A 6French (Fr) Pinnacle 10cm introducer sheath (Terumo Medical, Tokyo, Japan) was inserted in the right femoral artery over an 0.035 inch guidewire using the Seldinger technique. A 4Fr Angled Glidecath (Terumo Medical) was used to access and image the target vessel. Initial angiograms were performed by hand injections of 10ml of Ominipaque contrast (GE Healthcare). After injections, digitally subtracted roadmaps of the target vessel were constructed. A 0.014inch exchange length (300cm) Hi-Torque Wisper guidewire (Guidant, CA) was positioned across the target vessel through the 4Fr Angeled Glidecath. After removing the Glidecath, the Wisper wire was used to guide the thin film small vessel graft microdelivery catheter to the desired cerebral or femoral arteries. A 3Fr neurocatheter with a 0.60mm diameter push rod was used to deliver the small vessel graft. During the procedure heart rate, respiration rate, blood pressure, and oxygen saturation were monitored. The catheterization and small vessel graft implantation were visualized a continuous x-ray angiogram system (Philips Medical Systems, Andover, MA). All angiograms were recorded in single plane at 30 frames per second. After the final implantation, three dimensional angiograms with endoviews were constructed of the small vessel grafts.

5. RESULTS

Figure 3 shows the DSC plot of the NiTi thin film used for small vessel graft production. During heating one endothermic peak is observed corresponding to the transformation from martensitic to austenitic phase where the austenite start temperature is A_s = 22.09°C and the austenite finish temperature is A_f = 35.44°C. The A_f temperature is slightly below human body temperature. During cooling, two exothermic peaks are observed corresponding to the transformation from austenitic to intermediate rhombohedral phase, R-phase, and subsequently to the martensitic phase. The associated start and finish temperatures for these phases are R_s = 16.37°C, M_s = R_f = - 3.62°C and M_f = - 17.58°C. Figure 3 clearly demonstrates that both the A_f and A_s temperatures are in the range needed for heat activation of small vessel grafts in the vascular system as required for our small vessel graft design.

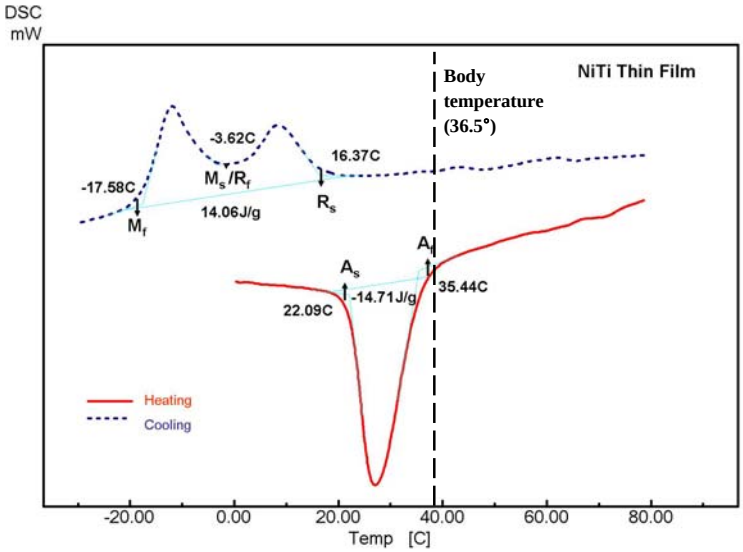

Fig. 3 DSC plot of superelastic NiTi thin film for small vessel graft construction

Stress-strain behavior for the NiTi thin film at 22°C and 35°C was also generated (Fig. 4). The tests at 22°C were conducted after cooling the film below M_f = -17.58°C, as such the film is entirely martensite. The Young's modulus of the film determined from the initial linear region is found to be 26.4GPa and the detwinning stress is 210MPa. After unloading the twin boundary motion produces a 0.032 residual strain. The initial linear stress-strain behavior of the film tested at 35°C produces a Young's modulus of 58.6GPa. The stress to induce the phase transformation from austenite to martensite is approximately 255MPa and a peak stress of 450MPa is applied without failure. Upon unloading, the material begins to reverse transform (i.e. from martensite back to austenite) at 210MPa and upon load removal there is approximately 0.003 strain present. The later strain may be attributable to the thin film slipping in the grips or permanent deformations near the grip region. These results demonstrate the pseudoleastic

response of the film at body temperature as well as twin boundary motion in the martensite phase (i.e. below body temperature during insertion into the catheter).

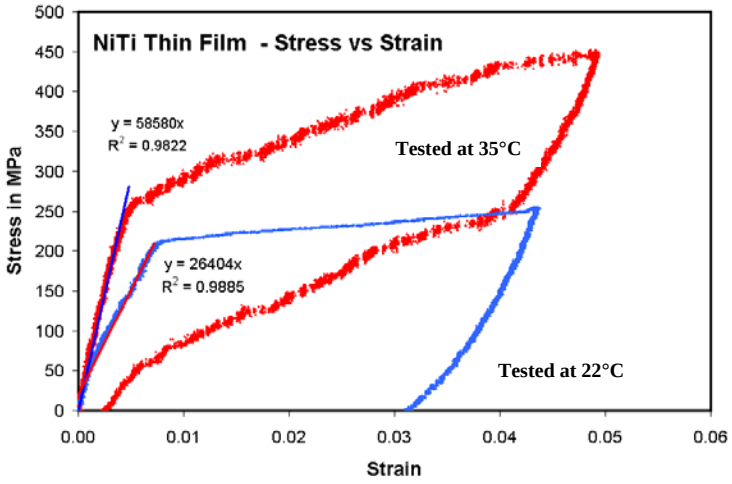

Fig. 4 Stress vs. strain behavior of superelastic NiTi thin film

In order to predict the biological response to NiTi thin film grafts, both the contact angle and surface topology of superelastic NiTi thin film was analyzed (Fig. 5). It has been previously demonstrated that NiTi's surface roughness and wettability have significant influence on its biological response [32-35]. Roughness measurements presented in Fig. 5 (A) indicate an average surface roughness of approximately 5nm. For comparison purposes, a commercial stent (Neuroform, Boston Scientific, MA) for neurovascular treatments was measured to have an average surface roughness of approximately 500nm, a value 100 times larger than NiTi thin film. Figure 5 (B) shows a picture of water droplet on the thin film to measure contact angle. The measured contact angle is 49.1° indicating nitinol surface is in the range of hydrophilic which is preferred for biological applications because these surfaces typically allow less fibrinogen adsorption and platelet adhesion reducing the thrombogenicity. In general, these results (Fig. 5 (A) and (B)) indicate that the thin film has an ultra smooth and hydrophilic surface to prevent adsorption of cells or protein molecules once implanted into the vascular system [16].

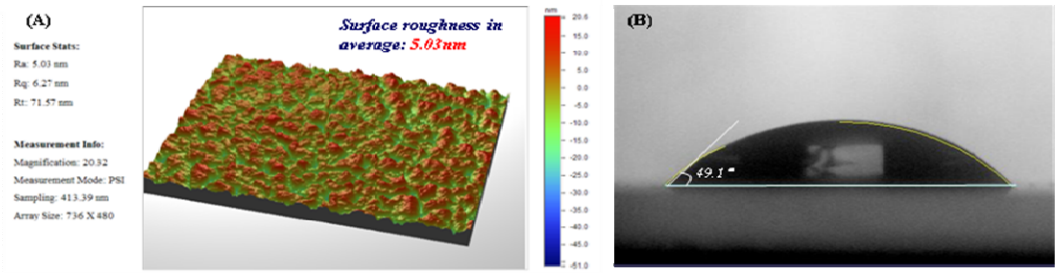

Fig. 5 (A) surface topology and (B) contact angle results of NiTi thin film small vessel graft

Figure 6 presents the experimental (data points) and theoretical results (Eq. (2)., solid line) for radial force of different thickness NiTi thin film grafts as well as double-wrapped NiTi thin film small vessel grafts. By quantifying the radial force of the various small vessel graft types, these results describe the ability of each small vessel graft to resist migration. The four thin film NiTi small vessel grafts (i.e., 6, 8, 10 and 12μm) exhibit radial forces of 0.0043N, 0.011N, 0.0261N, and 0.0427N, respectively. The theoretical predictions presented in Fig. 1 (B) agrees relatively well with the experimental data. Figure 6 also shows the force measurement results for a double-overlap design (i.e., 10μm thick film) doubles the radial force of its comparable single wrap counterpart. The single-zigzag and dual-zigzag wire reinforced segments (i.e., note these measurements are without film attached) produce radial forces of 0.031 and 0.070N respectively. These two structures when combined with a 10μm thick film exhibit 0.0781N and 0.0961N radial force respectively. The thin film small vessel grafts with a skeletal backbone produce radial forces 3~3.7times larger than a 10μm thin film graft by itself (i.e. without skeletal backbone). Although none of these small vessel grafts have enough force to treat stenoses, the NiTi thin film small vessel grafts should have sufficient force to immobilize the small vessel graft in small vessels to seat themselves in the vessels.

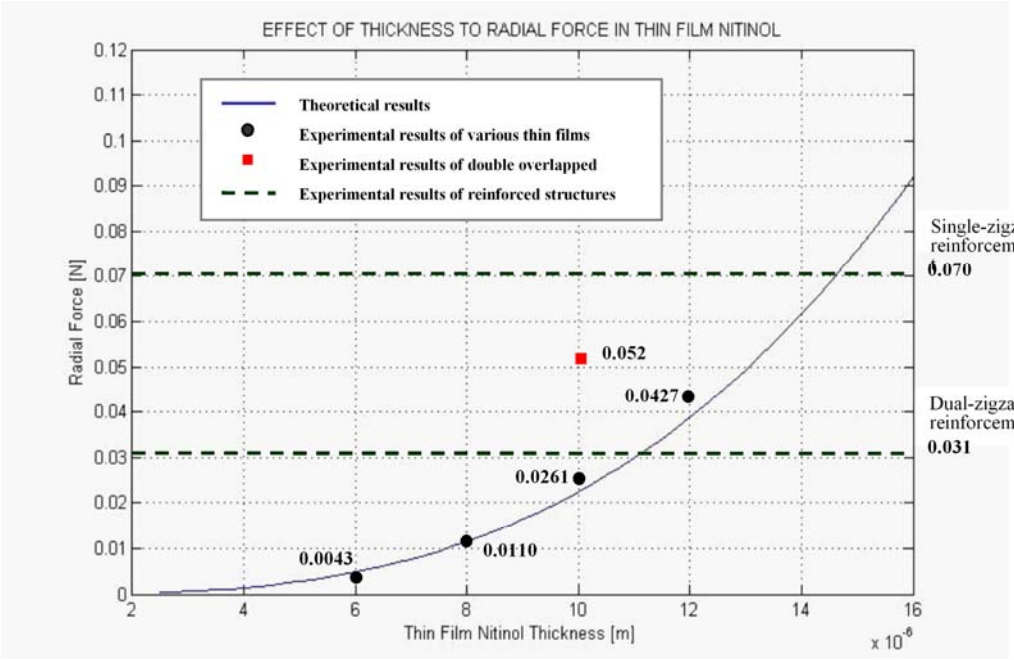

Fig. 6 Thickness vs. radial force of NiTi thin film small vessel graft

Stent stability was studied in the laboratory prior to animal testing. Figure 7 provides experimental and theoretical results for the different small vessel grafts studied in a flow loop. The ordinate lists the graft while the abscissa is the flow velocity at which small vessel graft migration occurs in tube diameters of 5mm. The thin film experimental results are represented by circular data points while theoretical

predictions are diamonds. There is qualitative agreement between the experimental and theoretical data but quantitative agreement is weak. This is attributed to the friction coefficient used in the analysis misrepresents the actual friction coefficient of the plastic tube. The 6 and 8μm thick films are immobilized at 0.5 and 0.65m/s velocities respectively; while the 10 and 12μm thick films show approximately 1.0 and 1.2m/s migration starting velocities. Thus, for typical body flows the 6~8μm thick films should only be used for lower velocity region (less than 0.5 and 0.65m/s) and 10~12μm thick films can be used for arteries in which flow velocities are in the range of 0.5~1.0m/s. The maximum velocity of each stent to be immobilized was calculated from Eq. (1) and presented as 0.15, 0.4, 0.87 and 1.43m/s respectively. This theoretical result shows linear tendency of frictional force by increase of flow velocity. However, the slopes from theoretical calculation and experimental data are most likely different because the assumed frictional coefficient is different from the actual coefficient.

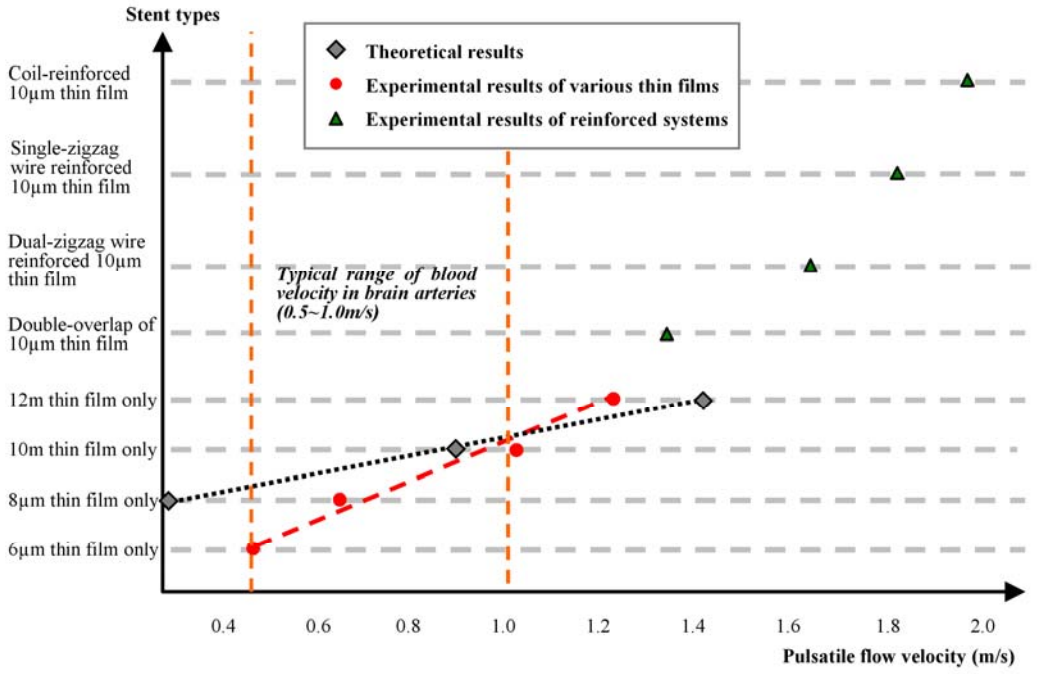

Fig. 7 Pulsatile flow velocity vs. migration starting velocities of thin film small vessel grafts

Figure 8 (A) shows clear visualization of the mechanically-clamped high contrast Td (tantalum) markers after implantation in the Maxillary and Lingual arteries in swine. For the 3~3.5mm diameter cerebral arteries, the theoretical blood flow velocity was 0.5m/s; thus, 6μm thick film grafts were implanted on the basis of the *in-vitro* stent-immobilization results. No migration occurred during the initial implantations. Endoviews derived from 180 degree angiograms (Fig. 8 (B)) showed that the internal profile (Fig. 8 (C)) of the region of graft implanted was smooth and without disturbance of the lumen by NiTi thin film small vessel grafts.

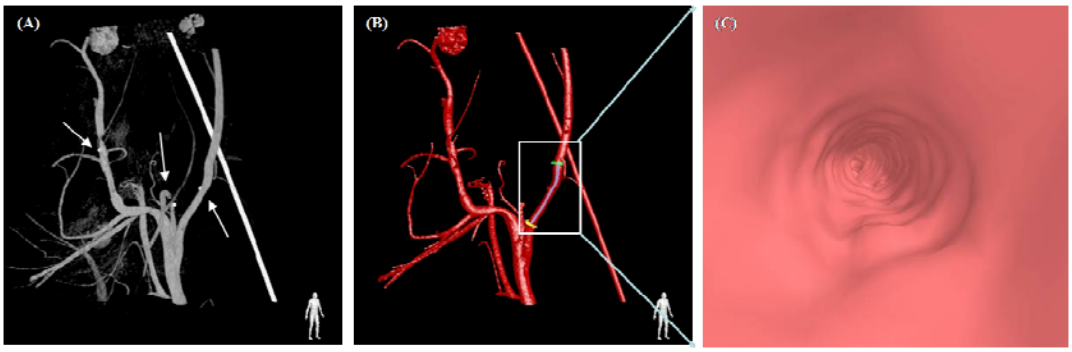

Fig. 8 Radiograph of implanted thin film NiTi small vessel graft: (A) visibility, (B) vascular structure of graft implanted, and (C) internal profile of swine's brain artery

In-vivo deployment test was also performed to evaluate the reinforced small vessel graft design. The swine's right femoral artery was selected as the target vessel for placement of thin film single-zigzag reinforced small vessel graft. Consecutive images in Fig. 9 (A) ~ (F) show sequential deployment of the small vessel graft during implantation. The small vessel grafts were easily deployed in 6seconds and thin film and wire structures were well placed in the artery. Angiograms demonstrated well positioned and deployed small vessel grafts which were easily visualized. All small vessel grafts were well apposed to the vascular wall in the desired location. No migration and unstable motion were observed during small vessel graft deployment. As for the non-reinforced thin film small vessel grafts, long-term animal testing will be needed to evaluate the performance of all small vessel graft designs before human applications can be considered.

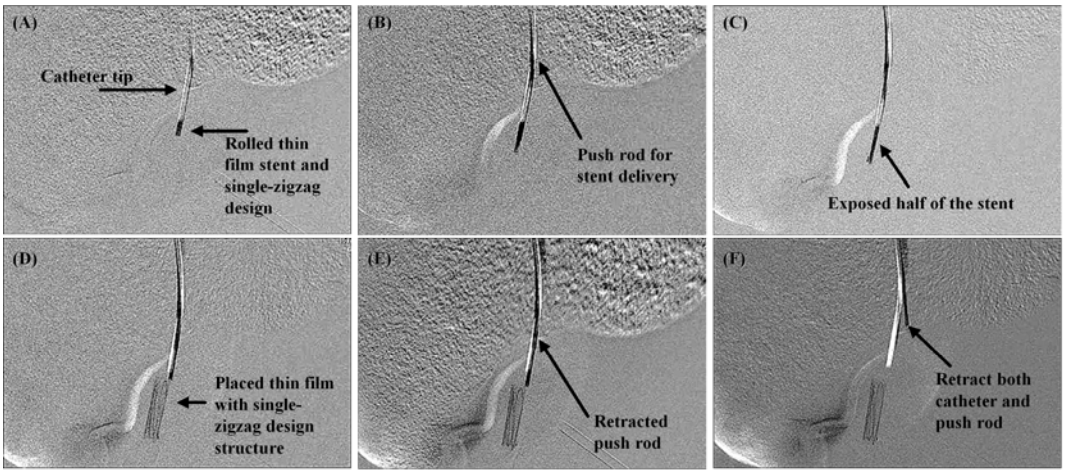

Fig. 9 Deployment of single-zigzag wire reinforced structure with NiTi thin film small vessel graft in Right Femoral artery of swine

Figure 10 (A) represents the angiogram demonstrating the placement of the NiTi thin film vessel graft and patency of the aorta two weeks after implantation. This preliminary *in-vivo* test in swine was performed to evaluate the feasibility of NiTi thin film small vessel graft for vascular repair. Angiography confirmed placement of the patterned thin film NiTi without any deformation and repeat angiography was performed to evaluate patency of the artery. Figure 10 (B) represents the SEM image of the grown endothelial layer through micro patterns on the film. This image showed uniformly spread-out endothelial layer covering lumen side of the vessel without thromobosis. In here, micro patterns promote endothelialization through holes from vessel wall to the lumen side.

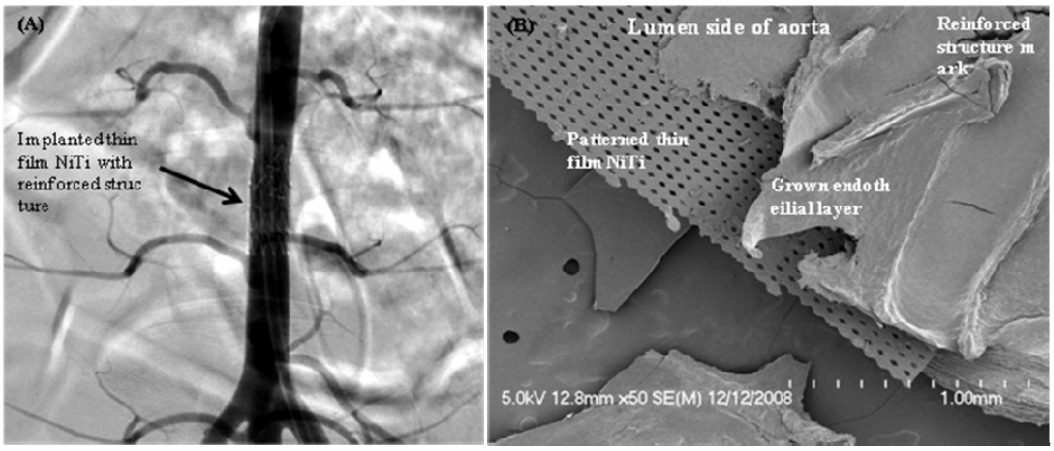

Fig. 10 (A) Patency of aorta after two weeks and (B) SEM image of the grown endothelial layer

Pathological studies were also performed in Fig. 11 to assess the endothelial cell growth through the 30x60μm diamond shaped patterns on NiTi thin film. Figure 11 (A) shows the small amount of neointimal proliferation observed in vessel walls where thin film NiTi covered compared with the uncovered region (Fig. 11 (B)). Organ tissue examination reveals the covering with thin film NiTi in implanting grafts shows absence of device associated abnormalities.

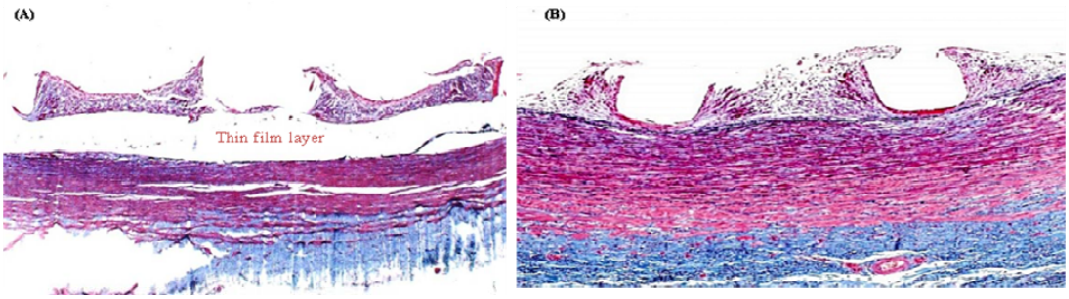

Fig. 11 Pathological results of the explanted aorta: (A) covered with NiTi thin film and (B) not covered with NiTi thin film

6. CONCLUSION

NiTi thin film small vessel grafts were manufactured and tested. Micro patterns are created using MEMS technology for promoting endothelial layer growth. Based on the analytical force calculations, the desired thin film thickness was determined and tested. Experimentally obtained values matched well with theoretical values which suggested that 10μm thick NiTi thin film will be required for small vessel graft stability. NiTi thin film small vessel grafts were shown to be appropriate for both *in-vivo* and *in-vitro* delivery to small blood vessels with very low profile delivery catheters. In acute animal experiments, small vessel grafts were easily visualized and delivered. *In-vivo* swine test results evaluated the placement and patency of the implanted stent by aorta angiogram. Harvested stent images demonstrated well-grown endothelial layer through micro patterns on the thin film and less neointimal proliferation compared with the bare stent implantation. Although animal studies are needed to determine the long term biological success of these devices, the NiTi thin film small vessel grafts could prove useful for a wide range of small vessel applications.

ACKNOWLEDGMENT

The authors would like to thank both the Telemedicine and Advanced Technology Research Center (TATRC) / Department of Defense under award number W81XWH-07-1-0672 and the Mattel Children;'s Hospital at UCLA Pediatric Translational Research Group for funding this research effort.

REFERENCES

[1] Shievink, WI., "Intracranial Aneurysms," N Engl J. Med, 336, 28-40 (1997).

[2] Huang, J. and van Gelder, JM., "The probability of sudden death from rupture of intracranial aneurysms: a meta-analysis," Neurosurgery, 51, 1101-1105 (2002).

[3] Brisman, JL., Song, JK., and Newell, DW., "Cerebral Aneurysms," N Engl J. Med, 355(9), 928-939 (2006).

[4] Guglielmi, G., Vinuela, F., Dion, J., and Duckwiler, G., "Electrothrombosis of saccular aneurysms via endovascular approach. Part2," J Neurosurg, 75, 8-14 (1991).

[5] Malisch, TW., Guglielmi, G., Vinuela, F., Duckwiler, G., Gobin, YP., Martin, NA., and Frazee, JG., "Intracranial aneurysms treated with the Guglielmi detachable coil: midterm clinical results in a consecutive series of 100 patients," J Neurosurg, 87(2), 176-183 (1997).

[6] Han, PP., Albuquerque, FC., Ponce, FA., Mackay, CI., Zabramski, JM., Spetzler, RF., and Mcdougall, DG., "Percutaneous intracranial stent placement for aneurysms," J Neurosurg, 99, 23-30 (2003).

[7] Lanzino, G., Wakhloo, AK., Fessler, RD., Hartney, ML., Guterman, LR., and Hopkins, LN., "Efficacy and current limitations of intravascular stents for intracranial internal carotid, vertebral, and basilar artery aneurysms," J Neurosurg, 91, 538-546 (1999).

[8] Wakhloo, AK., Lanzino, G., Lieber, BB., and Hopkins, LN., "Stents for intracranial aneurysms: the

beginning of a new endovascular era?," Neurosurgery, 43, 377-379.

[9] Lee, YJ., Kim, DJ., Suh, SH., Lee, SK., and Kim, DI., "Stent-assisted coil embolization of intracranial wide-necked aneurysms," Neuroradiology, 47, 680-689 (2005).

[10] Sani, S., Jobe, KW., Lopes, DK., "Treatment of wide-necked cerebral aneurysms with the Neuroform2 Treo stent," Nuerosurg Focus, 18(2), 1-5 (2005).

[11] Brisman, JL., Song, JK., Niimi, Y., and Berenstein, A., "Treatment options for wide-necked intracranial aneurysms using a self-expandable hydrophilic coil and a self-expandable stent combination," AJNR Am J Neuroradiol, 26, 1237-1240 (2005).

[12] Pumar, JM., Blanco, M., Vazquez, F., Castineira, JA., Guimaraens L., and Garcia-Allut, A., "Preliminary experience with Leo self-expanding stent for the treatment of intracranial aneurysms," AJNR Am J Neuroradiol, 26, 2573-2577 (2005).

[13] Higashida, RT., Halbach, V., Dowd, CF., Juravsky, L., and Meagher, S., "Initial clinical experience with a new self-expanding NiTi stent for the treatment of intracranial cerebral aneurysms: the Cordis Enterprise stent," AJNR Am J Neuroradiol, 26, 1751-1756 (2005).

[14] Turk, AS., Niemann, DB., Ahmed, A., and Aagaard-Kienitz, B., "Use of self-expanding stents in distal small cerebral vessels," AJNR Am J Neuroradiol, 28, 533-536 (2007).

[15] Ho, KK. and Carman, GP., "Sputter deposition of NiTi thin film shape memory alloy using a heated target," Journal of Thin Solid Films, 370, 18-29 (2000).

[16] Stepan, LL., Levi, DS., and Carman, GP., "A Thin Film NiTi Heart Valve," Journal of Biomechanical Engineering, 127(6), 915–918 (2005).

[17] Malek, AM., Alper, SL. and Izumo, SI., "Hemodynamic shear stress and its role in atherosclerosis," JAMA, 282(21), 2035-2042 (1999).

[18] David, NK., "Blood flow in arteries," Annu. Rev. Fluid Mech., 29, 399-434 (1997).

[19] Glagov, S., Zarins, C., Giddens, DP., and Kud, N., 1988, "Hemodynamics and atherosclerosis: insights and perspectives grained from studies of human arteries," Arch. Pathol. Lab. Med., 112, 1018-1031.

[20] Bell, RL., "Vascular Velocity Measurements in the Central Nervous System," Journal of Nuclear Medicine, 6, 1-6 (1965).

[21] Koc, RK., Akdemir, H., Menku, A., Okten IS., Selcuklu, A., and Tucer, B., "Evaluation of Cerebral Blood Flow Velocity with Transcranial Doppler Ultrasound in Central Nervous System Infections," Turkish Neurosurgery, 8, 76-81 (1998).

[22] Petrini, L., Migliavocca, F., Massarotti, P., Schievano, S., Dubini, G., and Auricchio, F., "Computational Studies of Shape Memory Alloy Behavior in Biomedical Applications," ASME J. of Biomech., 127, 716-725 (2005).

[23] Wu, Wei, Oi, Min, Liu, Xiao-Peng, Yang, Da-Zhi, and Wang, Wei-Qiang, "Delivery and release of NiTi stent in carotid artery and their interactions: A finite element analysis," Journal of Biomechanics,

40, 3034-3040 (2007).

[24] Ikeda, Seiichi, Arai Fumihilo, Fukuda, Toshio, Irie, Keiko, and Negoro, Makoto, "Three Dimensional Potoelastic Sress Analysis on Patient-Tailored Anatomical Model of Cerebral Artery," IEEE Proceedings of the 2004 International Symposium on Micro-Nano Mechatronics and Human Science, 145-150 (2004).

[25] Dunn, AC., Zaveri, TD., Keselowsky, BG., and Sawyer, WG., "Macroscopic Friction Coefficient Measurements on Living Endothelial Cells," Tribol. Lett., 27, 233-238 (2007).

[26] Jarrige, I., Holliger, P., and Jonnard, P., "Difussion processes in NiTi/Si, NiTi/SiO_2 and NiTi/Si_3N_4 systems under annealing," Thin Solid Films, 458, 314-321 (2004).

[27] Ken K. Ho, K. P. Mohanchandra and G.P Carman, "Examination of the sputtering profile of NiTi under target heating conditions," Thin Solid Films, 413, 1-7 (2002).

[28] Gill, JJ., Chang, DT., and Carman, GP., "Manufacturing issues of thin film NiTi microwrapper," Sensors and Actuators A, 93, 148-156 (2001).